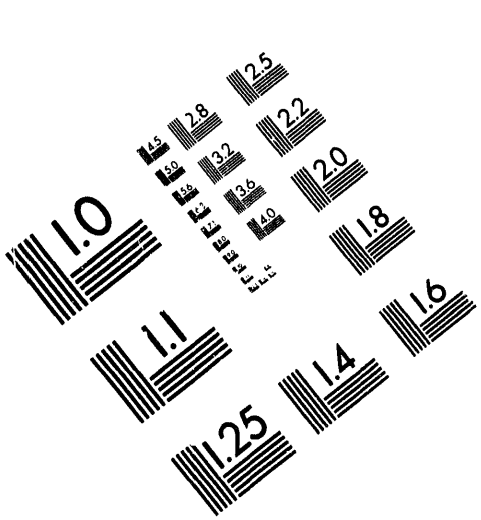



**Association for Information and Image Management**
1100 Wayne Avenue, Suite 1100
Silver Spring, Maryland 20910
301/587-8202

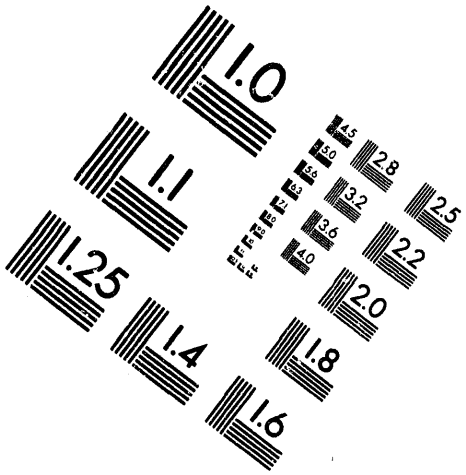

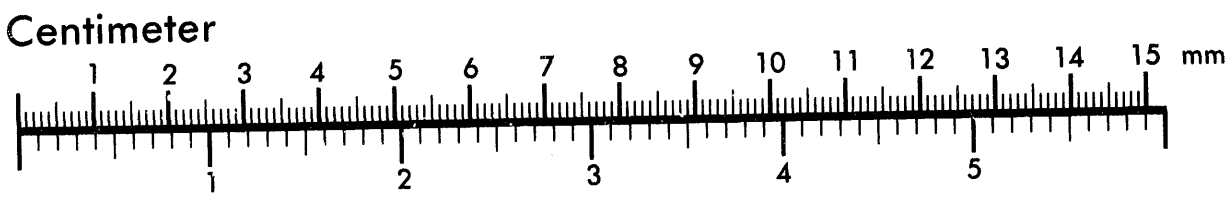


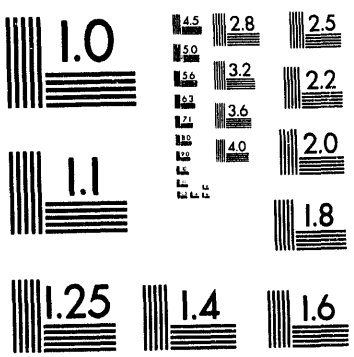

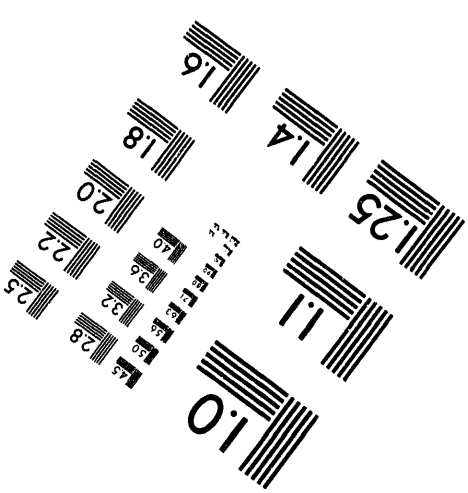

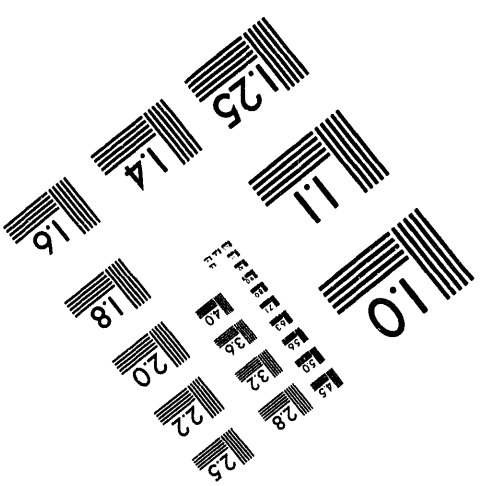

1 of 1

Conf-940416--22

PNL-SA-23487

# THE ROLE OF FRIT IN NUCLEAR WASTE VITRIFICATION

J. D. Vienna
D. A. Dorn
P. A. Smith
P. Hrma

April 1994

Presented at the
ACerS 96th Annual
Meeting and Exposition
April 24-28, 1994
Indianapolis, Indiana

Prepared for
the U.S. Department of Energy
under Contract DE-AC06-76RLO 1830

Pacific Northwest Laboratory
Richland, Washington 99352

# THE ROLE OF FRIT IN NUCLEAR WASTE VITRIFICATION.

JD Vienna*, PA Smith, DA Dorn, and P Hrma.
Pacific Northwest Laboratory[a], Richland, Washington 99352.

## ABSTRACT

Melter feed yield stress, viscosity and durability of frits and corresponding waste glasses as well as the kinetics of elementary melting processes have been measured. The results illustrate the competing requirements on frit. Four frits (FY91, FY93, HW39-4, and SR202) and simulated neutralized current acid waste (NCAW) were used in this study. The experimental evidence shows that optimization of frit for one processing related property often results in poorer performance for the remaining properties. The difficulties associated with maximum waste loading and durability are elucidated for glasses which could be processed using technology available for the previously proposed Hanford Waste Vitrification Plant.

## INTRODUCTION

Vitrification of nuclear waste requires additives which are often vitrified independently to form a frit. Frit composition is formulated to meet the needs of glass composition and processing.[1,2] The effects of frit on melter feed and melt processing, glass acceptance, and waste loading is of practical interest in understanding the trade-offs associated with the competing demands placed on frit composition.

Transport, mixing, and spreadability[3] of melter feed (which contain 15 volume % frit) is facilitated by low yield stress and viscosity. Melter feed rheology specifications have been imposed for the previously proposed Hanford waste vitrification plant (HWVP) that mandate an apparent viscosity below 700, 300, and 70 mPa.s at 10, 25, and 183 Hz, respecively, and a yield stress less than 10 Pa.[4] This specification is easily satisfied by modifying solids fraction in the melter feed slurry, provided that the frit particles behave hydrodynamically. However, the frits currently under consideration include compositions that are subject to phase separation and/or low durability. The composition / durability relationship for simple alkali-boro-silicate glasses was reported in literature.[5,6,7] The durability of these frits is strongly dependent on their position within the $R_2O$-$B_2O_3$-$SiO_2$ phase diagram and particularly on their position in or near the immiscibility dome.[8] Low durability can result in the leaching of the boron and alkali portions of the frit. Consequently, a hydrolyzed silica matrix is produced. Changes in temperature, mixing and pH can lead to increased gelation that increase yield stress and/or viscosity of the melter feed slurry. For this reason it is considered advantageous to use leach resistant frit.

---

[a] Pacific Northwest Laboratory is operated for the US DOE by Battelle Memorial Institute under contract DE-AC06-76RLO 1830.

Batch expansion (or foaming), which occurs due to the entrapment of evolved gasses within the cold cap, is reduced if the high viscosity ($10^3$ to $10^6$ Pa.s) melt temperature region does not coincide with that of gas evolution.[9] High viscosity melt formation is a function of frit viscosity and reactions between frit and waste. Excessive foaming decreases heat transfer to the cold cap, and thus decreases melting rate. However, some bubble evolution is beneficial for homogenization. A comparison of off gas volume and frit viscosity will yield an estimate of batch expansion (foaming) in the cold cap. Bubble formation and viscosity are described elsewhere.[10]

The viscosity/temperature relationship for glass must satisfy certain constraints for production of glass, i.e., a joule heated melter requires frit that provides lower viscosity glass (2 - 10 Pa.s at melting temperature). Heat transfer and mixing are attributed to convection in the melter which is dependent on viscosity. In addition, high viscosity will cause pouring problems. On the other hand, low viscosity (< 2 Pa.s), will promote refractory and electrode wear, and volatility.

Presently, glass acceptance rests upon the satisfaction of a 7-day product consistency test (PCT) criterion.[11] However, a more durable glass product is desirable provided that a processable glass composition is maintained.

To examine the interdependence of the above properties, four frits were tested. Two of these frits (FY91 and FY93) were optimized to form a 28 wt% neutralized current acid waste (NCAW) loaded glass with a processing temperature of 1150 °C. FY91 was designed for the highest glass durability with a viscosity of 6 Pa.s at 1150 °C using empirical models developed from a limited data base of glass properties.[12] This frit contains only three components $SiO_2$, $B_2O_3$, and $Li_2O$ (other components where found to be unnecessary for the optimization of glass properties alone). FY91 has been used in two melter runs; despite the high durability waste form produced, low melting rate and feed slurry rheology problems were observed and attributed to frit. The Integrated DWPF Melter System (IDMS) melter feed showed increased yield stress and viscosity that was attributed to FY91 frit induced gelling.[13] During the Kernforschungzentrum Karlsruhe (KfK) run,[b] cold cap spreadability was problematic and plugging occurred in the feed pipes. FY93 frit was designed (using more current models [14,15]) to achieve high durability while maintaining an easily processed glass. This frit includes a mixture of alkali and alkaline earth modifiers which are unnecessary for glass properties but may aid in processability by increasing frit durability.

The remaining two frits were not designed using property / composition models for NCAW, but have been established as standard frits for simulated nuclear waste vitrification. HW39-4 frit[16] was designed before property composition models were available and has been primarily used for glass development and melter testing. SR202 frit[17] was used at the DWPF for vitrification of Savannah River Waste.

## EXPERIMENTAL PROCEDURES

Simulated NCAW slurry was prepared according to procedures described by Smith et al.[18] Dry frit

---

b W. Grunewald, G. Roth, W. Tobie, S. Weisenburger, and K. Weiss, "Vitrification of Noble Metals Containing NCAW Simulant with and Engineering Scale Melter (ESM)," Campaign Report (1993).

(see Table I) was crushed to particle sizes between 75 and 175 μm (-80/+200 mesh). Frit, waste and recycle are then mixed with water to form a waste slurry consisting of 68.6% frit, 28.0% waste, and 3.4% recycle on a dry weight oxide basis. The solids loading of all these suspensions are 42 wt% which corresponds to approximately 20 vol% total solids including 15 vol% frit. These suspensions were digested by boiling for 2 h at 105 °C and aged in a 0.5 L vessel for four weeks under gentle agitation at 50 °C. An additional melter feed was produced with silica substituted for the frit using the same process.

Supernatant samples from the melter feed suspensions were analyzed by inductively coupled plasma spectroscopy (ICP) for Li. This value was used to calculate the fraction of the Li from frit dissolved in the melter feed suspension. This calculation underestimates the dissolution since no account of reprecipitation could be made. In addition, the suspension pH was measured during the aging process.

Rheological measurements were performed using a roto-viscometer with concentric cylinder geometry[c]. Rheograms were generated at a temperature of 50 °C by increasing the applied shear from 0 to 451 $s^{-1}$ using a 2-min ramp. The rheology data was fit to the Bingham equation:

$$\tau = \tau_0 + \eta_{pl}\,\dot{\gamma} \qquad (1)$$

where $\tau$ is the shear stress, $\tau_o$ is the yield stress, $\eta_{pl}$ is the plastic viscosity, and $\dot{\gamma}$ is the shear strain rate.

**Table I.** Frit and Glass Compositions Tested (in mass fractions). Each glass is comprised of 28 wt% waste, 3.4 wt% recycle (included in waste composition), and 68.6 wt% frit.

| | | FY 91 | | FY 93 | | HW 39-4 | | SR 202 | |
|---|---|---|---|---|---|---|---|---|---|
| Oxide | Waste | Frit | Glass | Frit | Glass | Frit | Glass | Frit | Glass |
| SiO2 | 0.0833 | 0.7230 | 0.5220 | 0.7400 | 0.5337 | 0.7000 | 0.5063 | 0.7700 | 0.5543 |
| B2O3 | 0.0001 | 0.2040 | 0.1399 | 0.1200 | 0.0823 | 0.1400 | 0.0960 | 0.0800 | 0.0549 |
| Na2O | 0.2365 | . | 0.0743 | 0.0600 | 0.1155 | 0.0900 | 0.1360 | 0.0600 | 0.1155 |
| Li2O | 0.0000 | 0.0730 | 0.0501 | 0.0600 | 0.0411 | 0.0500 | 0.0343 | 0.0700 | 0.0480 |
| CaO | 0.0074 | . | 0.0023 | 0.0100 | 0.0092 | 0.0100 | 0.0092 | . | 0.0023 |
| MgO | 0.0021 | . | 0.0007 | 0.0100 | 0.0075 | 0.0100 | 0.0075 | 0.0200 | 0.0144 |
| Fe2O3 | 0.2519 | . | 0.0791 | . | 0.0791 | . | 0.0791 | . | 0.0791 |
| Al2O3 | 0.0848 | . | 0.0266 | . | 0.0266 | . | 0.0266 | . | 0.0266 |
| ZrO2 | 0.1343 | . | 0.0422 | . | 0.0422 | . | 0.0422 | . | 0.0422 |
| Others* | 0.1997 | . | 0.0627 | . | 0.0627 | . | 0.0627 | . | 0.0627 |
| SUM | 1.0001 | 1.0000 | 0.9999 | 1.0000 | 0.9999 | 1.0000 | 0.9999 | 1.0000 | 1.0000 |

To measure feed microstructure during melting, the melter feed was dried at 120 °C, crushed, and heated in a gradient furnace in the temperature range from 620 to 1045 °C for one hour. Thin samples were polished and analyzed by optical microscopy. Feed melting stages, which include

---

[c] RV20 with M5 Measuring System and MV2 Sensor, Haake Instruments, Paramus, NJ.

sintering, bubble formation, batch expansion (also referred to here as foaming), bubble removal, and homogenization, were identified using methods described by Anderson et al.[19] In addition, the microstructure evolution of FY91 melter feed was measured as a function of heating time in a linear temperature gradient from 620 to 1045 °C for 22.5, 45, 90, 180, 360, and 720 min.

Glasses and frits listed in Table I were batched from oxides and carbonates, melted, crushed, and remelted in covered Pt/Rh crucibles. Subsequently, static dissolution and viscosity were measured. The normalized elemental releases were obtained by PCT for glasses and frits and by Materials Characterization Center (MCC-1) static leach test for frits. Viscosity was measured with a spindle viscometer from 950 to 1250 °C in 50 °C increments.

## RESULTS AND DISCUSSION

### Feed Processing

Figure 1 shows the rheological results of the melter feed with FY91 and SR202 frits. The rheology of the other melter feeds showed similar trends. However, large-scale testing with SR202 and HW39-4 in NCAW melter feeds have not been problematic whereas FY91 melter feeds have exhibited difficulties in pumping and cold cap spreading. Frit durability may provide some insight for the differences observed in the large-scale.

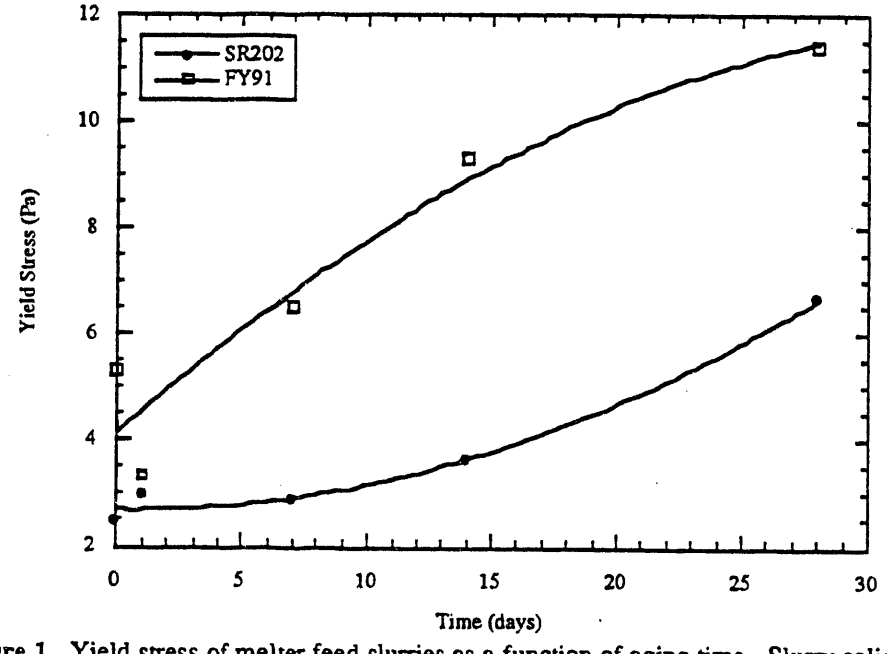


**Figure 1.** Yield stress of melter feed slurries as a function of aging time. Slurry solids concentration was held at nearly 500 g total oxide per liter, and pH is shown in Figure 2.

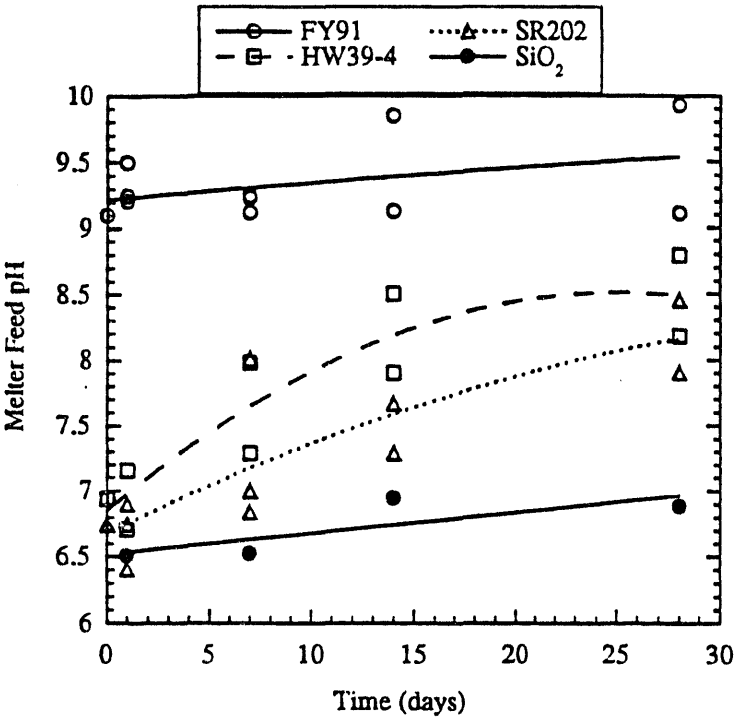


**Figure 2.** pH as a function of aging time for frit (and $SiO_2$) in melter feed slurry.

The effect of the frit dissolution on the melter feed is most easily observed by pH changes. Typically, the melter feed pH is approximately 6.5 at the time the frit is added. For the $SiO_2$ melter feed, only small changes in pH were observed during the aging period. The $SiO_2$ does not introduce any alkalies which can participate in any leaching or ion exchange reactions which raise pH. The FY91 melter feed increased to pH 9.1 during the melter feed digestion. Then, the pH of the FY91 melter feed slowly rises during the aging period. This pH change is attributed to frit dissolution which, in turn, is associated with the susceptibility to gelation. To further illustrate this point, the Li concentration in the melter feed supernatant liquid was measured as a function of aging (see Figure 3).

The FY91 frit showed that, minimally, 86% of the lithium in the frit was leached for four weeks of aging. In contrast, the SR202 and HW39-4 frits showed lithium fractions of 34 and 29% respectively, for 4 weeks of aging. In addition, the pH behavior of the SR202 and HW39-4 melter feeds showed much slower increases in pH and the final pH did not exceed 9. However, it is likely that the Li leaching and pH level for the HW39-4 and SR202 melter feeds would reach values similar to the FY91 melter feed if sufficient leaching time is allowed.

The measure of the frit behavior in the melter feed by Li fraction and pH may be considered uncertain due to the variety of components present and the complicated nature of the feed chemistry. Therefore, the frit durability was tested by PCT and MCC-1 tests. The results of the PCT tests on four frits (Table II) show that frits FY93 and HW39-4 dissolve in near congruent

amounts with respect to the normalized releases of B, Na, and Li ($r_B$, $r_N$, and $r_L$). FY91 frit showed a much higher $r_B$ and $r_L$, and dissolved nearly congruent. SR202 frit did not dissolve congruently. The boron of the SR202 dissolves more readily than the lithium and sodium components. For all of the frits, the silica shows a much lower concentration in solution compared with the other frit constituents.

**Table II.** MCC-1 and PCT results for each frit. Normalized releases are reported in $g/m^2$.28-day and $g/m^2$.7-day respectively.

| Normalized Release | FY91 | FY93 | HW39-4 | SR202 |
|---|---|---|---|---|
| MCC-1 Si | 266.13 | . | 78.65 | 34.69 |
| MCC-1 B | 2201.28 | . | 99.91 | 35.17 |
| MCC-1 Na | . | . | 98.08 | 35.94 |
| MCC-1 Li | 2448.49 | . | 98.93 | 32.26 |
| PCT Si | 2.52 | 3.04 | 2.29 | 1.67 |
| PCT B | 33.94 | 11.40 | 8.28 | 22.14 |
| PCT Na | . | 10.45 | 8.24 | 19.10 |
| PCT Li | 35.38 | 10.22 | 7.53 | 16.91 |

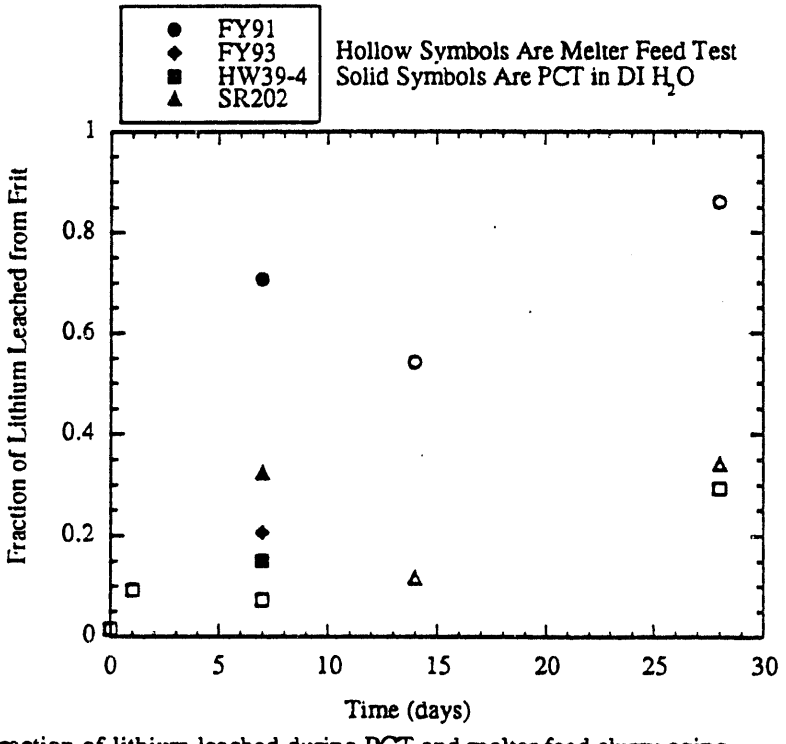


**Figure 3.** Fraction of lithium leached during PCT and melter feed slurry aging.

The normalized release data from the MCC-1 tests are listed in Table II for the frits HW39-4, FY91, and SR202. The releases for FY91 were much higher than the other frits. This behavior is similar to the PCT results. The MCC-1 release data showed that the HW39-4 frit was less durable

compared to the SR202 frit. These results were opposite to the PCT results. However, melter feed experience has shown that the HW39-4 and SR202 frits perform adequately with respect to rheology. Thus, the differences in the PCT and MCC-1 tests may not be important for the evaluation of frit for nuclear waste processing. More importantly, the amount of dissolution is an indicator of susceptibility to gelation. However, the relationship between frit durability and slurry rheology has not been well defined.

**Glass Processing**

A first-order model in ten component space shows the effect of composition and temperature on glass viscosity (h):

$$\ln \eta = \sum_{i=1}^{10} a_{Ai} g_i + \frac{\sum_{i=1}^{10} a_{Ei} g_i}{T - \sum_{i=1}^{10} a_{Ti} g_i} \qquad (2)$$

where T is absolute temperature, $g_i$ is mass fraction of the i-th component, $a_{Ai}$, $a_{Ei}$, and $a_{Ti}$ are the i-th component coefficients for A, E, and $T_0$ in the Fulcher model (Equation 3).[14] The A, E, and $T_0$ values obtained from measured glass viscosities (Figure 4) are listed along with those predicted using the first-order model in Table III. The relative order of the glass viscosities are: SR202 > FY93 > FY91 > HW39-4, as predicted.

$$\ln \eta = A + \frac{E}{T - T_0}, \qquad (3)$$

where A and E are constants and $T_0$ is the critical visco-elastic temperature.

Fulcher's model (Equation 3) is often used to represent glass viscosity over wide temperature ranges. Small errors can dramatically effect the prediction of low temperature viscosities if the temperature interval of measurement is narrow and far from $T_0$. Unfortunately, this is the case of frit viscosity measurements made for this study. The accuracy of low temperature viscosity extrapolation can be substantially improved by including a low temperature viscosity datum. Viscosity can be estimated at the frit sintering temperature by considering the strain rate / viscosity relationship. As neck formation becomes visible between adjacent frit particles, presumably 15% strain ($\varphi$) is achieved. This strain can be related to viscosity using Equation 4:

$$\varphi = \frac{\sigma t}{a \eta} \qquad (4)$$

where $\sigma$ is surface energy, t is time, and a is frit particle diameter.[20] Equation 4, and the measured sintering temperature were used to extend the frit viscosity data to lower temperatures (shown in Figure 5).

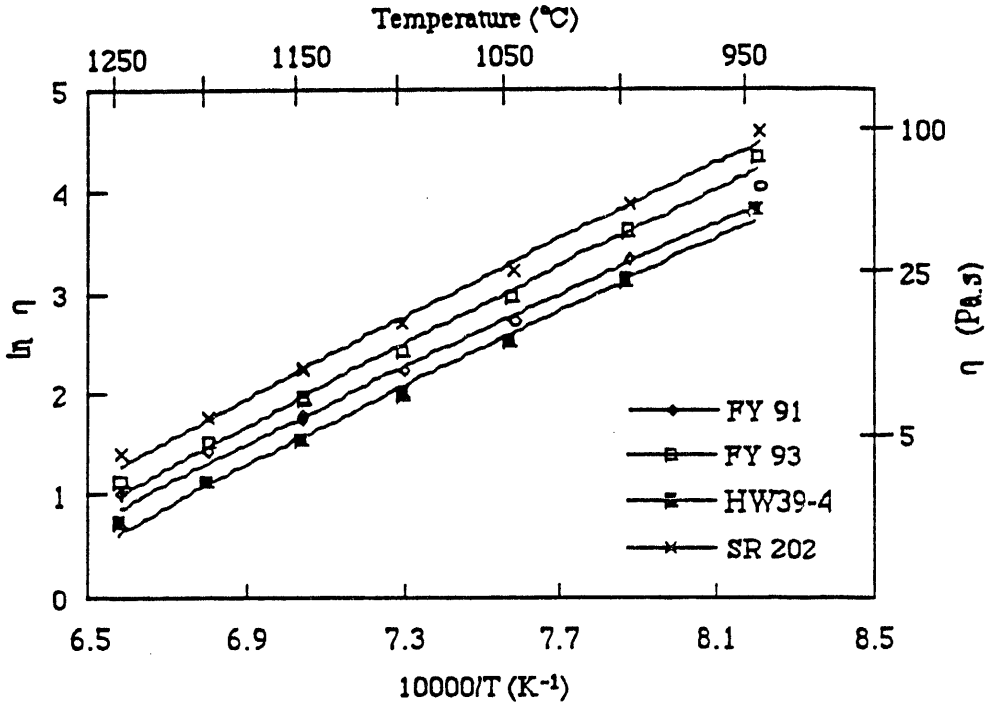


**Figure 4.** Glass viscosity vs. temperature.

**Table III.** Fulcher viscosity parameters measured from frits and glasses listed in Table I, and predicted for the same glass compositions.

| | A | E (K) | To (K) | η (Pa.s) |
|---|---|---|---|---|
| Measured Glass Viscosity Coefficients | | | | (at 1150 °C) |
| FY91 | -5.02 | 5,479 | 611 | 5.84 |
| FY93 | -5.93 | 6,817 | 554 | 6.84 |
| HW39-4 | -6.20 | 6,830 | 539 | 4.61 |
| SR202 | -6.15 | 7,696 | 501 | 9.00 |
| Predicted Glass Viscosity Coefficients | | | | |
| FY91 | -9.71 | 10,999 | 456 | 5.28 |
| FY93 | -8.33 | 9,915 | 467 | 7.73 |
| HW39-4 | -8.37 | 9,607 | 474 | 5.80 |
| SR202 | -7.83 | 9,651 | 463 | 9.20 |
| Measured Frit Viscosity Coefficients | | | | |
| FY91 | -5.87 | 7,860 | 556 | |
| FY93 | -7.81 | 10,112 | 503 | |
| HW39-4 | -5.42 | 6,467 | 609 | |
| SR202 | -4.95 | 7,054 | 607 | |

Theoretically, a low viscosity frit will aid in the formation of a thin well-spread cold cap. Frit viscosity is plotted as a function of temperature in Figure 5 for the four frits. The relative order of

increasing viscosity is SR202 > FY93 > FY91 > HW39-4.

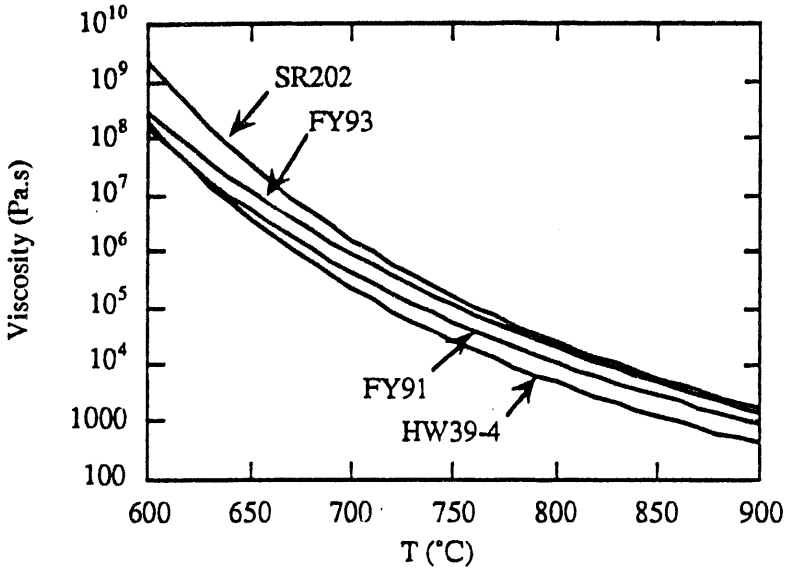


**Figure 5.** Frit viscosity vs. temperature generated by Fulcher extrapolation of measured viscosity data between 950 and 1250 °C.

Results from feed microstructure testing can be used to understand the effect of frit on the melting reactions. Microstructure evaluation tests allowed the evaluation of several melting stages by observing (using optical microscopy) samples that were heated in a constant temperature gradient (isothermal). Table IV summarizes this data for the four feeds heated in a gradient furnace for one hour.

The effect of time on each stage of cold cap melting was measured using microstructure analysis of feed samples. Table V summarizes the temperatures for each stage as a function of time. Generally, the characteristic temperatures for each melting stage decrease with increasing time.

Figure 6 illustrates the time and temperature dependence of each melting stage. The melting stages fit the Arrhenius model with a time constant ($\tau$) equal to the heating time. This is expected due to each stage's dependence on thermally activated processes (see Table VI). The extremely high activation energy required for the reactions indicates that a combination of many effects including diffusion, heat transfer, and reaction kinetics must be considered. In the case of sintering, the corresponding activity coefficient for viscous flow of frit is $2.5 \times 10^4$ K which is much lower that the $1.6 \times 10^5$ K from the Arrhenius equation. Lowering of frit viscosity by reactions with molten salts or other flux components from the waste resulted in the different activation energies. Hence, the presence of waste strongly accelerates the sintering of frit by reacting and forming a lower viscosity layer on the frit surface. The extremely high temperature coefficient for homogenization

cannot be explained by simple diffusion and must include other factors, such as convection. It is not yet known how frit composition effects the reaction rate with waste elements, but it is postulated that a frit with low viscosity will react more quickly. Data is widely scattered for the

**Table IV.** One hour Gradient Furnace Feed Microstructure Evaluation (MEG) Test Results for Each Feed.[d] Viscosity was extrapolated using high temperature frit viscosity data and the calculated viscosity at the sintering temperature.

| Stage | FY91 | FY93 | HW39-4 | SR202 |
|---|---|---|---|---|
| Temperature (°C) | | | | |
| Sintering (Necking) Begins | 612 | 622 | 612 | 641 |
| Bubble Formation Begins | 649 | 649 | 641 | 663 |
| Foaming Starts | 656 | 671 | 656 | 694 |
| Foaming Ends | 846 | 877 | 839 | 867 |
| Length of Foaming Interval | 190 | 206 | 183 | 173 |
| Last Undisolved Waste in Glass | >919 | 972 | 867 | >1058 |
| Frit Viscosity (MPa.s) | | | | |
| Bubble Formation Begins | 5.86 | 12.49 | 7.08 | 14.27 |
| Foaming Starts | 3.92 | 3.74 | 2.62 | 2.26 |

**Table V.** Gradient Furnace Feed Microstructure Evaluation (MEG) Test Results for FY91 Feed as a function of time.

| Time (h) | 22.5 | 45 | 90 | 180 | 360 | 720 |
|---|---|---|---|---|---|---|
| Temperature for each melting stage (°C) | | | | | | |
| Sintering (Necking) Begins | 623 | 614 | 612 | 609 | 600 | >600 |
| Bubble Formation Begins | 675 | 650 | 647 | 647 | 637 | 610 |
| Foaming Starts | 693 | 688 | 655 | 651 | 647 | 620 |
| Foaming Ends | 819 | 752 | 790 | 752 | 738 | 776 |
| Length of Foaming Interval | 126 | 64 | 135 | 101 | 91 | 156 |
| Last Undisolved Waste in Glass | 1004 | 970 | 977 | 963 | 953 | 943 |

**Table VI.** Arrhenius Fit to Melting Stages in FY91 Feed.

| $\ln \tau = A + B/T$ | A | B (K) |
|---|---|---|
| Sintering (Necking) Begins | -111.69 | 1.06E+05 |
| Bubble Formation Begins | -51.96 | 5.58E+04 |
| Foaming Starts | -37.01 | 4.20E+04 |
| Foaming Ends | -79.43 | 9.21E+04 |
| Last Undisolved Waste in Glass | -72.88 | 1.02E+05 |

d Viscosity Estimations were made using fitting Fulcher's model with high temperature viscosity data plus a calculated sintering viscosity. It was assumed that reactions between frit and waste did not significantly affect sintering temperature of frit.

end of foaming stage temperature. Two factors likely contribute to this large fluctuation: first, collapsing of a large bubble can have a large effect on the measured value; second, foam is very sensitive to experimental conditions and may be affected by mechanical or thermal influences while being removed from the furnace.

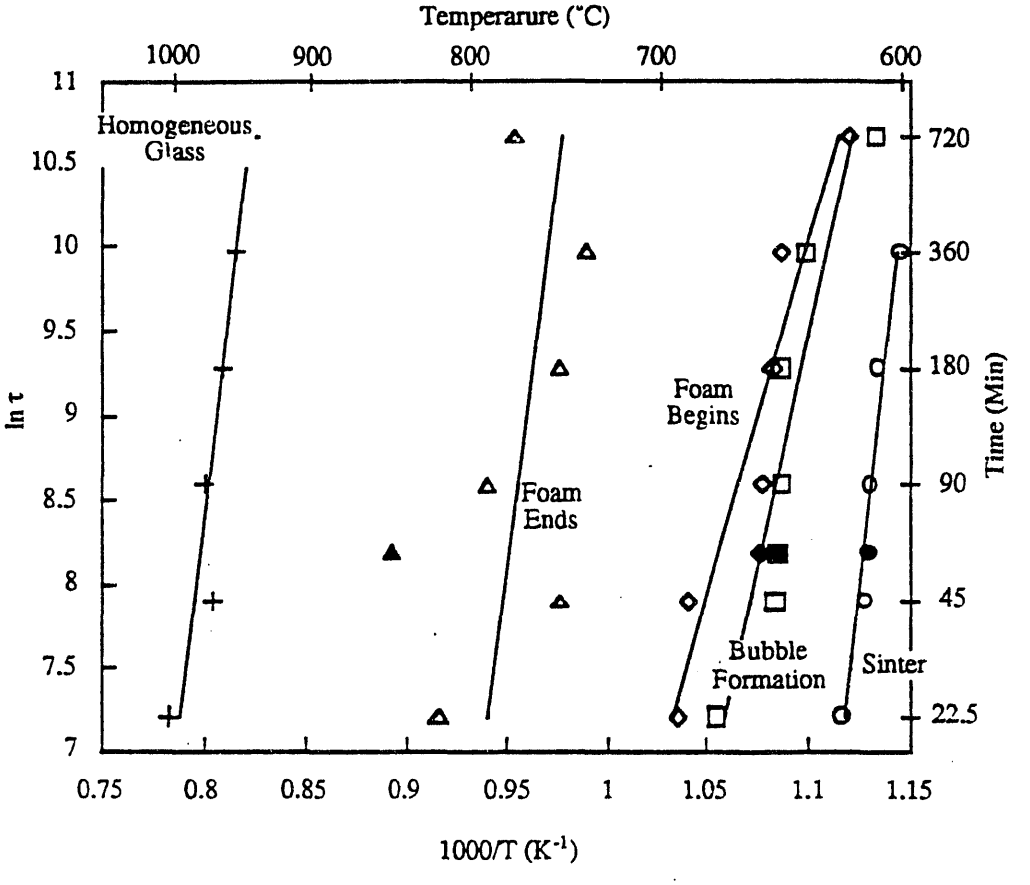


**Figure 6.** Arrhenius plot of melting stage evolution in FY91 feed. Solid characters correspond to one hour MEG which was conducted using a different temperature gradient and thus were not used to calculate fitted lines.

### Waste Form Acceptance

The normalized elemental releases by PCT are shown in Table VII for each glass. The normalized release of boron is the standard representation of waste glass dissolution. PCT release results showed the highest dissolution in HW39-4 waste glass followed by FY93 and SR202. FY91 provided the best glass in terms of PCT durability.

**Table VII.** Normalized Elemental Releases by PCT from Glass ($g/m^2$.7day). *Environmental Assessment (EA) glass produced using same procedures as other four glasses and the Defense Waste Processing Facility (DWPF) EA glass composition.

| Release | Si | B | Na | Li | pH |
|---|---|---|---|---|---|
| Measured | | | | | |
| FY91 | 0.26 | 0.65 | 0.42 | 0.62 | 9.83 |
| FY93 | 0.53 | 1.96 | 1.37 | 1.39 | 10.76 |
| HW39-4 | 0.73 | 3.86 | 2.63 | 2.51 | 11.40 |
| SR202 | 0.42 | 1.28 | 0.85 | 0.84 | 10.88 |
| EA-Glass* | 1.82 | 8.64 | 6.59 | 3.83 | 11.93 |
| Predicted | | | | | |
| FY91 | 0.31 | 1.62 | 0.90 | 1.43 | 9.84 |
| FY93 | 0.40 | 1.32 | 0.99 | 1.17 | 9.73 |
| HW39-4 | 0.47 | 2.16 | 1.66 | 1.72 | 10.75 |
| SR202 | 0.47 | 1.17 | 0.88 | 1.02 | 10.94 |
| EA-Glass* | 0.99 | 6.93 | 5.65 | 4.35 | 11.39 |

Normalized release from glass is related to composition according to the first-order model:

$$\ln r = \sum_{i=1}^{10} a_i g_i, \tag{5}$$

where r is the normalized release, $a_i$ is the i-th component coefficient, and $g_i$ is the i-th component mass fraction in a ten component glass ($SiO_2$, $B_2O_3$, $Na_2O$, $Li_2O$, CaO, MgO, $Fe_2O_3$, $Al_2O_3$, and all other components "Others"). The determination of $a_i$'s and more complete treatment of Equation 5 are given by Hrma, et al.[15] This model has been applied to the four glass compositions tested (see Table VII).

### Trade-Offs of Frit Formulation

A gain in feed and melter processability may be achieved by lowering durability or waste loading. Frit optimization has been put to practical use in maximized waste loading studies[21] and maximized durability.[12] These studies and their resultant frits were designed to maximize one of the competing demands on frit performance (glass waste loading or durability) while not considering demands such as frit dissolution. For example, the frit formulated for high waste loading is low in alkali and very refractory[21] (82 wt% $SiO_2$, 12 $B_2O_3$, and 6 $Li_2O$). This frit will be phase separated and will likely have low leach resistance. Because the frit is very refractory (82 wt% $SiO_2$) it may have melting problems similar to those seen with MEG testing of SR202 frit. The high durability glass obtained using FY91 frit came at the cost of difficulties in processing. Low leach resistance of this frit appeared to have created rheology problems which caused pumping difficulties and incomplete cold cap spreading. Generally, frits designed for high NCAW loading or very high durability will have low alkali content which promotes phase separation and has been found to degrade durability.

## CONCLUSIONS

More durable frits may be less susceptible to rheological difficulties in melter feed testing based on melters tests as well as experimental evidence. Four measurements to assess the durability of frit were presented: PCT, MCC-1, pH monitoring, and Li leaching in melter feed. The results of all these tests were in good agreement. Hence, inexpensive test such as PCT and MCC-1 are capable of indicating frit dissolution behavior in laboratory melter feed experiments.

Little difference was seen in the viscosity and melting stages of the two frits HW39-4 and FY91 based on laboratory tests. However, melter tests showed slower melting with FY91 feeds. This suggests that cold cap spreading has a stronger influence on the melting rate of NCAW feeds than feed reactions. Frit reaction with molten salts from waste appears to lower viscosity at the surface of frit particles, and thus enhance frit sintering.

Frits designed for maximum waste loading and maximum durability will minimize alkali content in frit. This change will likely lower frit durability (due to phase separation) and increase susceptibility to gelation in the melter feed.

## ACKNOWLEDGEMENTS

The authors would like to acknowledge the assistance of MJ Schweiger, DE Smith, and S Palmer for a majority of glass testing, DS Kim for numerous insightful conversations and guidance, DE Larson for programmatic guidance. DA Dorn would like to acknowledges partial support from the Department of Energy (DOE), Division of University and Industrial Programs, Office of Energy Research, as a Science and Engineering Research Semester program participant at Pacific Northwest Laboratory.

## REFERENCES

1 P. Hrma, "Processing Constraints on High-Level Nuclear Waste Glasses for Hanford Waste Vitrification Plant," Proceedings of the 1993 International Conference on Nuclear Waste Management and Environmental Remediation, Vol. 1, ASME, NY, 403-9 (1994).

2 P. Hrma and R. J. Robertus, "Waste Glass Design Based on Property Composition Functions," Ceram. Eng. Sci. Proc. 14 [11-12], 187-203 (1993).

3 D. D. Yasuda and P. Hrma, "The Effect of Slurry Rheology on Melter Cold Cap Formation," In Ceramic Transactions, Nuclear Waste Management IV, Eds. G. G. Wicks, D. F. Bickford, L. R. Bunnell, 23, 349-59 (1991).

4 J. Kalia, "Hanford Waste Vitrification Plant Project Technical Data Package," WHC-SD-HWV-DP-001, Rev. 6-6, Westinghouse Hanford Company (1994).

5 D. E. Clark and B. K. Zoitos, Corrosion of Glass, Ceramics and Ceramic Superconductors, Noyes Publications, Park Ridge, NJ (1992).

6 R. H. Doremus, "Chemical Durability of Glass," in Glass II, Treatise on Materials

Science and Technology, M. Tomozawa and R. H. Doremus eds. Vol 17 (1979).

7 M. B. Volf, Chemical Approach to Glass, Glass Science and Technology, Vol 7, Elsevier, NY (1984).

8 D. K. Peeler and P. R. Hrma, "Predicting Liquid Immiscibility in Multi-component Nuclear Waste Glasses," Ceramic Transactions, This Volume (1994).

9 D. S. Kim and P. Hrma, "Volume Changes During Batch to Glass Conversion," *Ceram. Bulletin*, **69** [6], 1039-43 (1990).

10 D. Kim and P. Hrma, "Laboratory Studies for the Estimation of Melting Rate in Nuclear Waste Glass Melters," Ceramic Transactions, This Volume (1994).

11 "Waste Acceptance Product Specifications For Vitrified High-Level Waste Forms." US DOE-EM Report (1993).

12 R. A. Watrous, O. L. Kruger, P. Hrma, and J. M. Perez, Jr., "Recycle Stream Impacts on Feed Treatment Flow sheets and Glass Formulation for the Hanford Waste Vitrification Plant," Nuclear Waste Management IV, Advances In Ceramics, Am. Ceram. Soc. 321-32 (1992).

13 N. D. Hudson, "Integrated DWPF Melter System Campaign Report: Hanford Waste Vitrification Plant (HWVP) Process Demonstration," US-DOE Report WSRC-TR-92-0403, Westinghouse Savannah River Company (1992).

14 P. Hrma, G. F. Piepel, D. E. Smith, P. E. Redgate, and M. J. Schweiger, "Effect of Composition and Temperature on Viscosity and Electrical Conductivity of Borosilicate Glasses for Hanford Nuclear Waste Immobilization," Ceramic Transactions Vol 39, Am. Ceram. Soc., Westerville, OH (1994).

15 P. R. Hrma, G. F. Piepel, M. J. Schweiger, and D. E. Smith, "First-Order Model For Durability of Hanford Waste Glasses as a Function of Composition," Proceedings of the 3rd International Conference on High Level Radioactive Waste Mgt., 1236-43 (1992).

16 R. W. Goles and R. K. Nakaoka, "Hanford Waste Vitrification Program Pilot Scale Ceramic Melter Test 23," Pacific Northwest Laboratory Report PNL-7142 (1990).

17 N. D. Hutson, J. R. Zamecnik, M. E. Smith, D. H. Miller, and J. A. Ritter, "Integrated DWPF Melter System (IDMS) Campaign Report: The First Two Noble Metals Operations (U)," WSRC-TR-91-400, Defense Waste Processing Technology, Savannah River Laboratory, Aiken, SC (1991).

18 P. A. Smith, M. H. Langwoski, S. M. O'Rourke, and K. McDonald, "The Effect of Formic and Nitric Acid on Simulated Neutralized Current Acid Waste Rheology," Ceramic Transactions, This Volume (1994).

19 L. D. Anderson, T. Dennis, M. L. Elliott, and P. Hrma, "Waste Glass Melting Stages," Ceramic Transactions Vol 39, Am. Ceram. Soc., Westerville, OH (1994).

20 G. W. Scherer, "Viscous Sintering Under a Uniaxial Load," *J. Am. Ceram. Soc.*, 69 [9] C-206,7 (1986).

21 P. T. Fini and P. Hrma, "Optimization of Waste Loading In Simulated Neutralized Current Acid Waste (NCAW) Glasses," Ceramic Transactions, This Volume (1994).

DATE
FILMED
8/24/94

END